Nanoscale Res Lett (2006) 1:167–171
DOI 10.1007/s11671-006-9010-z

NANO EXPRESS

Electronic structures of GaAs/$Al_xGa_{1-x}As$ quantum double rings

Shu-Shen Li · Jian-Bai Xia

Published online: 11 August 2006
© to the authors 2006

Abstract In the framework of effective mass envelope function theory, the electronic structures of GaAs/Al_x-$Ga_{1-x}As$ quantum double rings (QDRs) are studied. Our model can be used to calculate the electronic structures of quantum wells, wires, dots, and the single ring. In calculations, the effects due to the different effective masses of electrons and holes in GaAs and $Al_xGa_{1-x}As$ and the valence band mixing are considered. The energy levels of electrons and holes are calculated for different shapes of QDRs. The calculated results are useful in designing and fabricating the interrelated photoelectric devices. The single electron states presented here are useful for the study of the electron correlations and the effects of magnetic fields in QDRs.

Keywords Electronic structures · GaAs · Quantum double rings · Nanostructures · Effective-mass theory · Band mixing

PACS: 78.20.Bh · 78.66.Fd

Introduction

Growth of semiconductor nanostructures has attracted much attention due to their unique electronic and optical properties as well as potential applications in making electronic and optoelectronic devices.

S.-S. Li (✉) · J.-B. Xia
State Key Laboratory for Superlattices and Microstructures, Institute of Semiconductors, Chinese Academy of Sciences, 912, Beijing 100083, People's Republic of China
e-mail: sslee@red.semi.ac.cn

Recently, T. Mano et al. fabricated the self-assembled formation of concentric quantum double rings (QDRs) with high uniformity and excellent rotational symmetry using the dropletepitaxy technique [1]. They calculated the electronic energy levels using the effective mass approximation. For computational purposes, they assumed that the quantum rings have a rotational symmetry relative to the growth axis. Aside from this assumption, no adjustable parameters were used in the model. However, the valence band mixing was not considered in their calculations.

We have studied the electronic states and valence band structures of the InAs/GaAs quantum single ring [2]. In this letter, using the effective-mass envelope-function theory, we will study the electron and hole states of QDRs. In our calculations, the effects due to the different effective masses of electrons and holes in GaAs and $Al_xGa_{1-x}As$ and the valence band mixing are included. Our model can be used to calculate the electronic structures of quantum wells, wires, dots and the single ring. The single electron states are useful for the study of the electron correlations and the effects of magnetic fields on QDRs.

Theoretical model

Figure 1 shows the schematic plot of the GaAs/Al_xGa_{1-x} As QDRs. In the following, we choose z-direction of our coordinate system to be perpendicular to the plane of quantum rings. The QDRs are concentric. We suppose the inner radius and outer radius are R_1, R_2 for the small ring and R_3, R_4 for the large ring, respectively. The height of QDRs is l. If $R_1 = R_2$, or $R_3 = R_4$, the QDRs become quantum single ring.

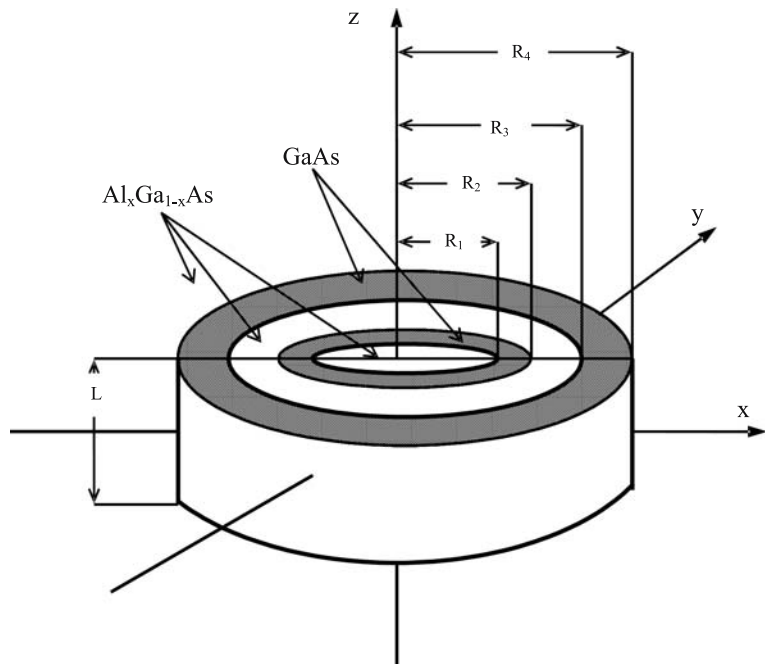

Fig. 1 Schematic plot of the GaAs/$Al_xGa_{1-x}As$ quantum double rings

According to Burt and Foreman's effective-mass theory and taking into account the difference of the effective-masses between GaAs and $Al_xGa_{1-x}As$ [3, 4], the electron Hamiltonian can be written as (neglecting the second- and higher-order terms in the approximation)

$$H_e = \mathbf{P}\frac{1}{2m_e^*(x,y,z)}\mathbf{P} + V_e(x,y,z). \tag{1}$$

In the above equation,

$$m_e^*(x,y,z) = \begin{cases} m_1^* & R_1^2 \le \rho^2 \le R_2^2 \text{ or } R_3^2 \le \rho^2 \le R_4^2, \text{and} |z| \le l, \\ m_2^* & \text{others}, \end{cases} \tag{2}$$

$$V_e(x,y,z) = \begin{cases} 0 & R_1^2 \le \rho^2 \le R_2^2 \text{ or } R_3^2 \le \rho^2 \le R_4^2, \text{and} |z| \le l, \\ E_c & \text{others}, \end{cases} \tag{3}$$

where $\rho^2 = x^2 + y^2$, and m_1^* and m_2^* are the effective electron masses in GaAs and $Al_xGa_{1-x}As$, respectively. E_c is the conduction band offset between GaAs and $Al_xGa_{1-x}As$. The electron Schrödinger equation is

$$H_e\Psi_e(\mathbf{r}_e) = E_e\Psi_e(\mathbf{r}_e). \tag{4}$$

Using the periodic boundary condition, we assume that the electron wave functions have the following forms

$$\Psi_e(\mathbf{r}) = \frac{1}{L^{3/2}}\sum_{n_x n_y n_z} a_{n_x n_y n_z} e^{i(k_{nx}x + k_{ny}y + k_{nz}z)}, \tag{5}$$

with $k_{ni} = k_i + n_i K$, $n_i = 0, \pm1, \pm2, \ldots$, and $i = x,y,z$; $K = 2\pi/L$, $\mathbf{r} = (x, y, z)$. L denotes the periods of the large units. The matrix elements of Hamiltonian (1) for Eq. 5 can be written as

$$\left(\frac{\hbar^2}{2m_2^*}\delta + \frac{\hbar^2}{2m_{12}^*}S_iS_j\right)\left(k_{nx}k'_{nx} + k_{ny}k'_{ny} + k_{nz}k'_{nz}\right) + \left(\delta - S_iS_j\right)E_c, \tag{6}$$

where $k'_{ni} = k_i + n'_i K$, and

$$\delta = \begin{cases} 1 & \text{for } n_x = n'_x,\ n_y = n'_y, \text{ and } n_z = n'_z, \\ 0 & \text{otherwise}, \end{cases} \tag{7}$$

$$\frac{\hbar^2}{2m_{12}^*} = \frac{\hbar^2}{2m_1^*} - \frac{\hbar^2}{2m_2^*}, \tag{8}$$

$$S_i = \begin{cases} l/L, & n_z = n_z^*, \\ \frac{\sin[\pi(n_z - n'_z)l/L]}{\pi(n_z - n'_z)}, & n_z \ne n'_z, \end{cases} \tag{9}$$

$$S_j = \begin{cases} \pi[(R_2^2 - R_1^2) + (R_4^2 - R_3^2)]/L^2, & n_x = n'_x \text{ and } n_y = n'_y, \\ (F_2 - F1 + F_4 - F_3)/(\lambda L), & n_x \ne n'_x \text{ or } n_y \ne n'_y. \end{cases} \tag{10}$$

In the above equation, $F_i = R_i J_1(\lambda K R_i)$ with $i = 1,2,3,4$; J_1 is the first-order Bessel function $J_1(x) = \frac{x}{2\pi}\int_0^\pi \cos(x\cos\theta)\sin^2\theta\, d\theta$; and $\lambda = \sqrt{(n_x - n'_x)^2 + (n_y - n'_y)^2}$. Therefore, we can calculate the electronic states from Eq. 6.

For the hole states, the hole effective mass Hamiltonian can be written as [4]

$$H_h = \frac{1}{2m_0}\begin{bmatrix} P_+ & R & -Q_- & 0 \\ R^\dagger & P_- & C^\dagger & -Q_+^\dagger \\ -Q_-^\dagger & C & P_- & -R \\ 0 & -Q_+ & -R^\dagger & P_+ \end{bmatrix} + V_h, \quad (11)$$

where

$$V_h(\mathbf{r}) = \begin{cases} 0 & R_1^2 \le \rho^2 \le R_2^2 \; or \; R_3^2 \le \rho^2 \le R_4^2, \; and \; |z| \le l, \\ V_{h0} & \text{otherwise}, \end{cases} \quad (12)$$

$$\begin{aligned} P_\pm &= p_x(\gamma_1 \pm \gamma_2)p_x + p_y(\gamma_1 \pm \gamma_2)p_y + p_z(\gamma_1 \mp 2\gamma_2)p_z, \\ Q_\pm &= 2\sqrt{3}\left[(p_x \pm ip_y)\sigma p_z + p_z\pi(p_x \pm ip_y)\right], \\ R &= \sqrt{3}\left[(p_x + ip_y)\mu(p_x + ip_y) - (p_x - ip_y)\gamma(p_x - ip_y)\right], \\ C &= 2p_z(\sigma - \pi)(p_x - ip_y) - 2(p_x - ip_y)(\sigma - \pi)p_z, \end{aligned} \quad (13)$$

and

$$\begin{aligned} \sigma &= (-1 - \gamma_1 + 2\gamma_2 + 6\gamma_3)/6, \\ \pi &= (1 + \gamma_1 - 2\gamma_2)/6, \\ \gamma &= (\gamma_2 + \gamma_3)/2, \\ \mu &= -(\gamma_2 - \gamma_3)/2. \end{aligned} \quad (14)$$

Here γ_1, γ_2, and γ_3 are functions of x, y, and z,

$$\gamma_1, \gamma_2, \gamma_3 = \begin{cases} \gamma_{11}, \gamma_{12}, \gamma_{13} & for \; R_1^2 \le \rho^2 \le R_2^2 \\ & or \; R_3^2 \le \rho^2 \le R_4^2, \; and \; |z| \le l, \\ \gamma_{21}, \gamma_{22}, \gamma_{23} & \text{otherwise}. \end{cases} \quad (15)$$

The notations γ_{11}, γ_{12}, γ_{13} and γ_{21}, γ_{22}, γ_{23} are the Luttinger effective mass parameters of GaAs, $Al_xGa_{1-x}As$ materials, respectively; and m_0 is the free electron mass.

The hole envelope function equation is

$$H_h\Psi_h = E_h\Psi_h. \quad (16)$$

Using the normalized plane-wave expansion method [5], we assume that the hole-wave functions have the following form:

$$\Psi_h(\mathbf{r}_h) = \frac{1}{L^{3/2}}\sum_{n_xn_yn_z}\begin{bmatrix} a_{n_xn_yn_z} \\ b_{n_xn_yn_z} \\ c_{n_xn_yn_z} \\ d_{n_xn_yn_z} \end{bmatrix} e^{i(k_{nx}x + k_{ny}y + k_{nz}z)}. \quad (17)$$

The matrix elements of Hamiltonian (11) for Eq. 17 can be written as

$$\begin{aligned} (P_\pm)_{n_xn_yn_z,n'_xn'_yn'_z} &= (\gamma_\pm^1\delta + \gamma_\pm^2 S_iS_j)(k_{nx}k'_{nx} + k_{ny}k'_{ny}) \\ &\quad + (\gamma_\pm^3\delta + \gamma_\pm^4 S_iS_j)(k_{nz}k'_{nz}), \\ (Q_\pm)_{n_xn_yn_z,n'_xn'_yn'_z} &= 2\sqrt{3}\{[(\sigma_2 - \delta_2)\delta \\ &\quad -(\sigma_1 - \delta_1 - \sigma_2 + \delta_2)S_iS_j]\} \\ &\quad (k'_{nx} \pm ik'_{ny})k'_{nz}.+[\pi_2\delta - (\pi_1 - \pi_2)S_iS_j]\} \\ &\quad (k_{nx} \pm ik_{ny})k'_{nz}\}, \\ R_{n_xn_yn_z,n'_xn'_yn'_z} &= \sqrt{3}\{[\mu_2\delta - (\mu_1 - \mu_2)S_iS_j](k_{nx} + ik_{ny}) \\ &\quad (k'_{nx} + ik'_{ny}) - [\gamma^2\delta - (\gamma^1 - \gamma^2)S_iS_j] \\ &\quad (k_{nx} - ik_{ny})(k'_{nx} - ik'_{ny})\}, \\ C_{n_xn_yn_z,n'_xn'_yn'_z} &= 2(\sigma_1 - \delta_1 - \pi_1 - \sigma_2 + \delta_2 + \pi_2)S_iS_j \\ &\quad \left[(k_{nx} - ik_{ny})k'_{nz} - (k'_{nx} - ik'_{ny})k_{nz}\right], \\ (V_h)_{n_xn_yn_z,n'_xn'_yn'_z} &= (\delta - S_iS_j)V_{h0}, \end{aligned}$$

with $\gamma_\pm^1 = \gamma_{21} \pm \gamma_{22}$, $\gamma_\pm^2 = (\gamma_{11} \pm \gamma_{12}) - \gamma_\pm^1$, $\gamma_\pm^3 = \gamma_{21} \mp 2\gamma_{22}$, $\gamma_\pm^4 = (\gamma_{11} \mp 2\gamma_{12}) - \gamma_\pm^3$, $\sigma_i - \delta_i = (-1 - \gamma_{i1} + 2\gamma_{i2} + 6\gamma_{i3})/6$, $\pi_i = (1 + \gamma_{i1} - 2\gamma_{i2})/6$, $\gamma^i = (\gamma_{i2} + \gamma_{i3})/2$, $\mu_i = -(\gamma_{i2} - \gamma_{i3})/2$, $\sigma_i - \delta_i - \pi_i = (-1 - \gamma_{i1} + 2\gamma_{i2} + 3\gamma_{i3})/3$, and $i = 1$ or 2. Thus, the hole energy levels can be worked out from Eq. 18.

Results and discussion

We take the material parameters from Ref. 6. The aluminum proportion in $Al_xGa_{1-x}As$ is taken to be $x = 0.3$, which equals the value for the experimental samples in Ref. 1. The effective masses and band gaps E_g^Γ(eV) are listed in Table 1. The conduction-band offset is assumed to be 65% of the band gap difference.

We have calculated the electron and hole energy levels as functions of the radius of QDRs. In calculations, we assume the height of QDRs to be l=3 nm.

Figure 2a, b shows the electron and hole energy levels as a function of R_1, respectively, for fixed

Table 1 The effective masses and band gaps E_g^Γ (eV) of bulk GaAs and $Al_{0.3}Ga_{0.7}As$

Material	$m_e^*(m_0)$	γ_1	γ_2	γ_3	$E_g^\Gamma(eV)$
GaAs	0.067	6.98	2.06	2.93	1.519
AlAs	0.15	3.76	0.82	1.42	3.099
$Al_{0.3}Ga_{0.7}As$	0.0919	6.014	1.688	2.477	1.993

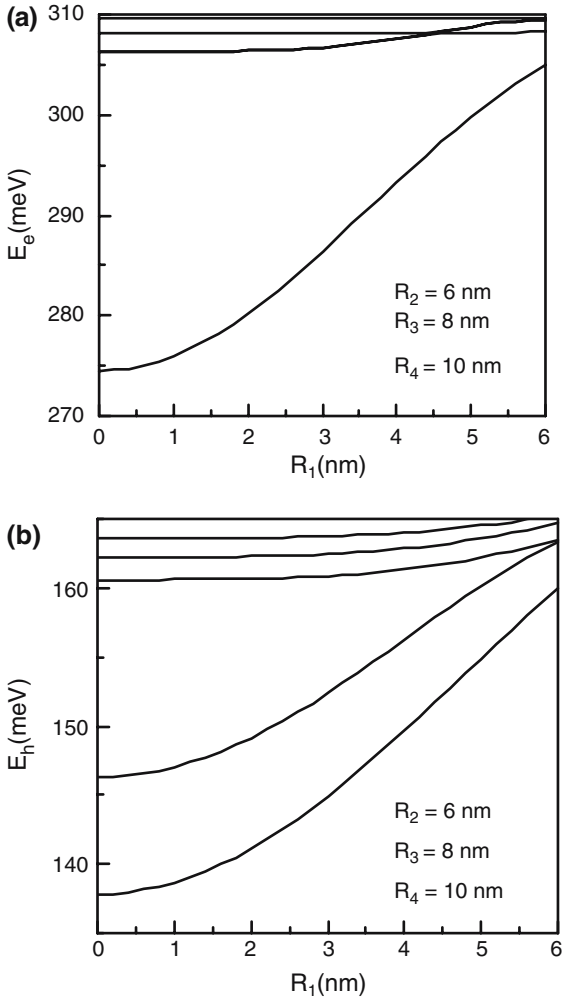

Fig. 2 The electron (**a**) and hole (**b**) energy levels as a function of R_1 for R_2=6 nm, R_3=8 nm, and R_4=10 nm

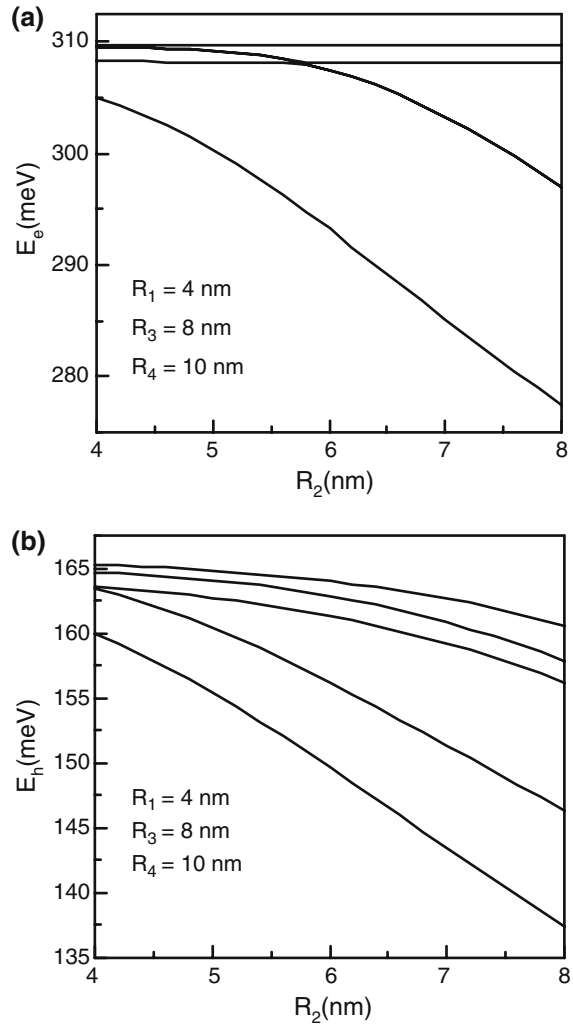

Fig. 3 The electron (**a**) and hole (**b**) energy levels as a function of R_2 for R_1=4 nm, R_3=8 nm, and R_4=10 nm

R_2 = 6 nm, R_3=8 nm, and R_4=10 nm. From Fig. 2a, one may find that there is only one deep confined electronic energy level for the above structure parameters. The anti-crossing is found near R_1=4.5 nm for the second and the third electron energy levels. Figure 2b shows there are two confined hole energy levels for the above structure parameters.

Figure 3a, b shows the electron and hole energy levels as a function of R_2, respectively, for R_1=4 nm, R_3=8 nm, and R_4=10 nm. The one and two confined electron energy levels is found for $R_2 <$ and > 5.9 nm, respectively. The anti-crossing is found near the same R_2=5.9 nm for the second and the third electron energy levels. The hole confined energy levels decrease monotonical as R_2 increases.

Figure 4a, b shows the electron and hole energy levels as a function of R_3, respectively, for R_1=4 nm, R_2=6 nm, and R_4=10 nm. The one and two confined electron energy levels is found for $R_3 <$ and > 8.1 nm, respectively. The anti-crossing is found near the same R_2=8.1 nm for the second and the third electron energy levels. The only two confined hole energy levels is found for $R_3 > 9.5$ nm.

Figure 5a, b shows the electron and hole energy levels as a function of R_4, respectively, for R_1=4 nm, R_2=6 nm, and R_3=8 nm. The one and two confined electron energy levels is found for $R_4 <$ and > 10 nm, respectively. The anti-crossing is found near the same R_4=10 nm for the second and the third electron energy levels. The only two confined hole energy levels is found for $R_4 <$ 8.8 nm,

Taking the structure parameters of the QDRs to be l = 3.5 nm, R_1=10 nm, R_2=35 nm, R_3=40 nm, and R_4=60 nm, the transition energies for the ground electron energy level transiting to the ground heavy- and light-hole energy levels were calculated to be 1.694, and 1.696 eV, respectively. These calculated

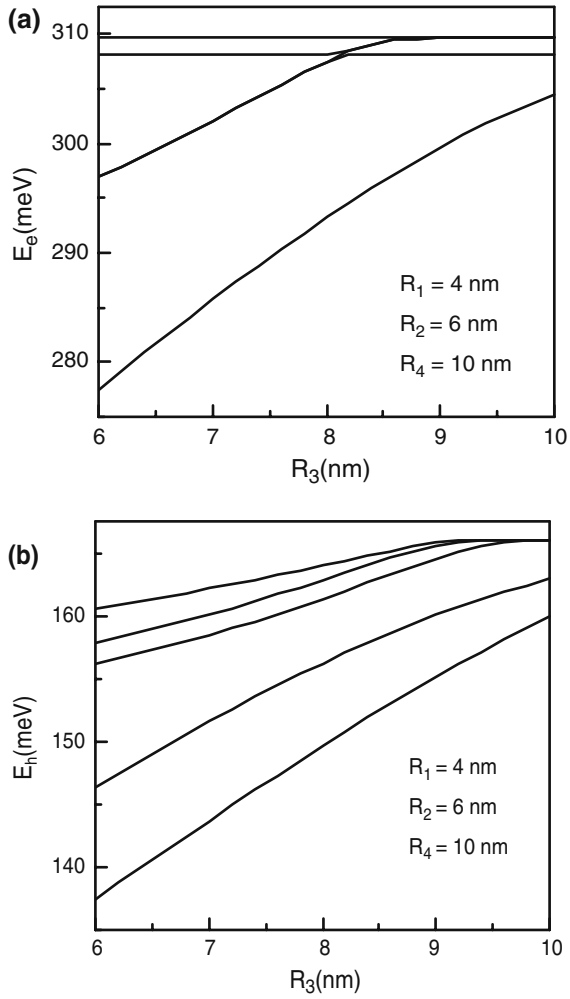

Fig. 4 The electron (**a**) and hole (**b**) energy levels as a function of R_3 for R_1=4 nm, R_2=6 nm, and R_4=10 nm

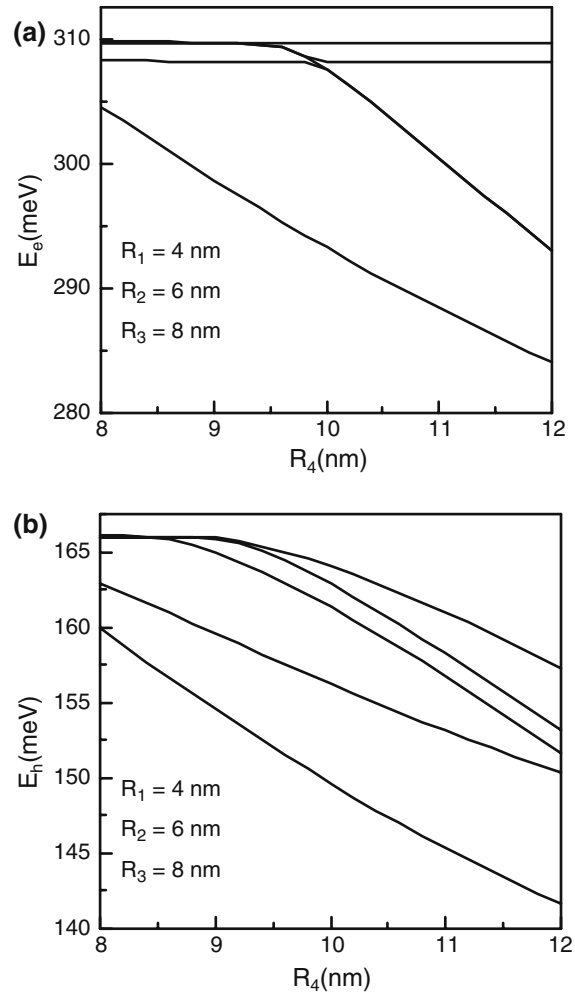

Fig. 5 The electron (**a**) and hole (**b**) energy levels as a function of R_4 for R_1=4 nm, R_2=6 nm, and R_3=8 nm

results are somewhat higher than the available experimental data in Ref. 1 for we have not included the binding energy of exciton. The exciton binding energy is estimated to be 15 meV from the difference between the theoretical values and experimental data.

Summary

In this paper, we have calculated the electronic states of GaAs/$Al_xGa_{1-x}As$ QDRs. The model we proposed can be used to calculate the electronic states of quantum wells, wires, dots, and the single ring. The single electron states are useful for the study of the electron correlations and the effects of magnetic fields on QDRs. Our calculated results are useful in designing and fabricating the interrelated photoelectric devices.

Acknowledgments This work was supported by the National Natural Science Foundation of China and the Special Foundations for State Major Basic Research Program of China (Grant No. G2001CB309500).

References

1. T. Mano, T. Kuroda, S. Sanguinetti, T. Ochiai, T. Tateno, J. Kim, T. Noda, M. Kawabe, K. Sakoda, G. Kido, N. Koguchi, Nano Lett. **5**, 425 (2005)
2. S.-S. Li, J.-B. Xia, J. Appl. Phys. **89**, 3434 (2001) and J. Appl. Phys. **91**, 3227 (2002)
3. M.G. Burt, J. Phys. Condens. Matter **4**, 6651(1992)
4. B.A. Foreman, Phys. Rev. B **52**, 12241(1995)
5. M.A. Cusack, P.R. Briddon, M. Jaros, Phys. Rev. B **54**, 2300 (1996)
6. I. Vurgaftmana, J.R. Meyer, J. Appl. Phys. **89**, 5815 (2001)